Fast and Furious: Fluid's not Hot

Aparajithan Venkateswaran David Stearns

Nicholas Johnston

Adam Norris

APPM 4650, Summer 2018

University of Colorado, Boulder

Abstract

In this project we examine the behavior of fluid as it flows along a heated plate. As the fluid flows along the plate, it is slowed down due to friction. This leads to the formation of the momentum boundary layer. Further, due to the difference in temperature, the fluid is heated, which leads to the formation of a thermal boundary layer. We study these boundary layers in detail.

We first use the conservation of mass, momentum and energy to develop a system of partial differential equations. We then perform a similarity transform to turn the system into ordinary differential equations. We convert this boundary value problem into an initial value problem using root finding techniques. This makes our model amenable to conventional integration schemes like Runge-Kutta. The model we develop here is robust enough to accommodate fluids possessing different properties.

1 Introduction

Only math nerds would call 2^{500} *finite.*

– Leonid Levin

The properties of fluids are key in many areas of physics, aerodynamics, and chemistry. In this project, we will explore some of these properties. Particularly, we will study the flow of a fluid over a heated plate. When fluid flows close to a plate, it is slowed down by kinetic friction; however, far away from the plate this phenomenon does not occur. This results in a steadily increasing boundary layer where the fluids are significantly slowed down. This also

forces some of the fluid upward due to conservation of mass and momentum. Furthermore, if the plate is heated, then the temperature of the fluid will gradually increase as it flows across the plate. This results in another boundary layer known as the thermal boundary layer, and it behaves similarly to the momentum boundary layer. These boundary layers depend on the properties of the fluid.

The laws of nature dictate that mass, momentum and energy be conserved. This will form the basis of our mathematics as we model this seemingly simple phenomenon. The goal of this project is to develop a robust model that allows us to study the momentum and thermal boundary layers for different fluids.

The rest of the report is organized as follows: In Section 2, we will present the problem scenario in detail. In Section 3, we will develop a simple mathematical model that describes the problem while accounting for a few nuances. In Section 4, we will create techniques that help us address practical issues with our model. Section 5 will present and discuss the solutions of our model, while delving deeper into the physics. Finally, Section 6 will conclude our discussion.

2 Problem Statement

Physics is becoming too difficult for the physicists.

– David Hilbert

In this problem, a fluid flows along a stationary flat plate. Initially, before the fluid comes in contact with the plate, it has an initial non-zero horizontal velocity. At this time, the fluid's *velocity profile* is uniform, i.e. all "layers" of the fluid have the same horizontal velocity. Further, the velocity of the fluid has no vertical component.

Now, as the fluid flows along the stationary plate, friction comes into play. As a result of friction, the layer of the fluid closest to the plate "sticks" and comes to rest. As the fluid continues to flow, the next closest layer also comes to rest. This reduction in horizontal velocity propagates through the fluid's velocity profile as the fluid flows further along the plate. With this knowledge, we can draw a *momentum boundary layer* that traces the closest layer of the fluid that still has the same initial horizontal velocity. We are interested in studying this momentum boundary layer.

At this point, we must remember that mass is conserved. However, because of friction, the

outgoing mass flux is smaller than the incoming mass flux. It stands to reason that some of the fluid gets "pushed" upwards i.e., there is an *induced vertical velocity*. We must account for this vertical velocity when we find the momentum boundary layer.

To make the problem more interesting, let us consider making the plate hot. Therefore, the initial temperature of the fluid is smaller than the temperature of the plate. For the sake of simplicity, let us assume that the temperature of the plate is uniformly held at a constant value. Similar to the velocity profile, we can construct a *temperature profile* for the fluid. Before touching the plate, the temperature profile is uniform.

Since the plate is hotter than the fluid, heat moves from the plate to the fluid by the second law of thermodynamics. When the fluid touches the plate, the layer of the fluid closest to the plate increases in temperature. As the fluid flows along the plate, heat moves along the fluid making subsequent layers of the fluid hotter. By tracing the closest layer of the fluid that still has the same initial temperature, we can construct a *thermal boundary layer*. The second item of interest in this problem is the thermal boundary layer.

3 Model

All models are wrong, but some are useful.

– George E. P. Box

We are interested in studying the momentum and thermal boundary layers of the fluid as it flows along a stationary plate held at a constant temperature. Therefore, we need to know the velocity and temperature at different points along the fluid's profile as it flows along the plate.

First, we will setup the coordinate system. We will define the y-axis as the left-most edge of the plate and the x-axis as the top edge of the plate. With this coordinate system in mind, let the horizontal velocity be u and the vertical velocity be v. Let the temperature be T. Finally, let the kinematic velocity of the fluid be ν and the thermal diffusivity of the fluid be α. Let the initial horizontal velocity be U_∞, initial temperature of the fluid be T_∞, and the temperature of the plate be $T_w > T_\infty$.

Now, from the conservation of mass, x-momentum, and energy, respectively, we have the following coupled system of partial differential equations, known as the *boundary layer equations*:

$$u_x + v_y = 0 \tag{1}$$

$$uu_x + vu_y = \nu u_{yy} \tag{2}$$

$$uT_x + vT_y = \alpha T_{yy} \tag{3}$$

We can define some initial and boundary conditions for the system above. From the way we defined the problem in Section 2, we know that the fluid should have horizontal velocity U_∞ and temperature T_∞. Therefore,

$$T(0, y) = T_\infty, \quad u(0, y) = U_\infty, \quad v(0, y) = 0 \tag{4}$$

Along the plate, the fluid should have zero horizontal velocity and the same temperature as the plate. Therefore,

$$T(x, 0) = T_w, \quad u(x, 0) = 0, \quad v(x, 0) = 0 \tag{5}$$

Finally, far from the plate, the temperature and the horizontal velocity should reach the initial values. However, we do not know anything about the vertical velocities. Therefore,

$$T(x, \infty) = T_\infty, \quad u(x, \infty) = U_\infty \tag{6}$$

To solve this system of partial differential equations, we can perform a similarity transformation to convert it into a coupled system of ordinary differential equations. We introduce the following variables:

$$u = U_\infty F'(\eta) \tag{7}$$

$$v = \frac{1}{2}\sqrt{\frac{\nu U_\infty}{x}}\,[\eta F'(\eta) - F(\eta)] \tag{8}$$

$$G(\eta, Pr) = \frac{T - T_\infty}{T_w - T_\infty} \tag{9}$$

where the similarity variable η is,

$$\eta = \frac{y}{\sqrt{\frac{\nu x}{U_\infty}}} \tag{10}$$

and the Prandtl number $Pr = \nu/\alpha$. After performing the transformation, we can reduce the coupled system defined in Equations (1–3) into:

$$F''' + \frac{1}{2}FF'' = 0 \tag{11}$$

$$G'' + \frac{Pr}{2}FG' = 0 \tag{12}$$

subject to the following boundary conditions,

$$F(0) = 0 \tag{13}$$

$$F'(0) = 0 \tag{14}$$

$$F'(\infty) = 1 \tag{15}$$

$$G(0) = 1 \tag{16}$$

$$G(\infty) = 0 \tag{17}$$

Notice that Equation (11) depends only on η, which depends on ν (kinematic viscosity). Therefore, we can deduce that this equation is the transformed version of Equations (1–2) in the original system i.e., it represents the conservation of mass and x-momentum. Similarly, Equation (12) is the transformed version of Equation (3) in the original system. This is

indicated by the dependence on Pr, which depends on α (thermal diffusivity). Thus, this equation represents the conservation of energy.

There are two interesting things about the new system. Firstly, note that F can be solved independently of G using Equation (11). Thus, ideally, we can solve F first and then use that to solve G.

Secondly, if we set $Pr = 1$, observe that Equation (11) and (12) look almost identical. Thus, when $Pr = 1$, we can expect F' and G to behave identically. We can use this fact to verify the solutions we calculate.

$$(F')'' + \frac{1}{2}F(F')' = 0$$
$$(G)'' + \frac{1}{2}F(G)' = 0$$

4 Handling a Boundary Value Problem

The boundary condition of the universe is that it has no boundaries.

– Stephen Hawking

While we have a good model, our model contains a boundary value problem. Unfortunately, we do not, yet, know how to solve a boundary value problem. Therefore, we have to create an algorithm to convert this boundary value problem into an initial value problem.

One way to convert this into an initial value problem is to guess the missing initial conditions such that they lead to the boundary conditions. Therefore, we first estimate the initial condition $F''(0) = k_1$ and adjust k_1 such that we get $F'(\infty) = 1$. This is a relatively simple task because F can be solved independently of G. Notice that this is a root finding problem, and we can use root finding techniques to find the initial guess.

Once we have an initial guess for F'', we can employ a similar root finding technique to guess the initial condition $G'(0) = k_2$ such that $G(\infty) = 0$. Observe, from the system, that k_2 depends on both our initial guess $F''(0) = k_1$, and the Prandtl number Pr. k_1 is independent of everything else. Therefore, we need to change our guess $G'(0) = k_2$ whenever we change the Prandtl number Pr.

Pr	$F''(0)$	$\infty_{F'}$	$G'(0)$	∞_G
0.1			-0.14718171	25
0.2			-0.18520988	25
0.5			-0.25929849	20
1	0.33205735	10	-0.33205735	10
2			-0.42230815	10
5			-0.57668870	8
10			-0.72814051	8

Table 1: *Initial guesses of $F''(0)$ and $G'(0)$ for different Prandtl numbers Pr. Here, we numerically integrated with a step size, $h = \Delta\eta = 0.1$. The different values of ∞ (the upper bound for integration) are also shown.*

The problem with this guess and check approach is that we have to numerically integrate up to ∞. But, we do not actually have to evaluate the system at ∞. This is due to the fact that both, F' and G asymptotically approach constant numbers. Thus, after a certain point, these values converges to the asymptotes. This convergence gives us a sign that further integration will yield no significant changes.

With these initial conditions, we can now solve the coupled system using familiar integration techniques. In particular, we will use the fourth-order Runge-Kutta integration scheme.

5 Results

Any inaccuracies in this index may be explained by the fact
that it has been sorted with the help of a computer.

– Donald Knuth

We first guessed the initial conditions by constructing a root finding problem described in Section 4. Using bisection method, we found $F''(0) = 0.33205735$[1]. This value is fixed for all Prandtl numbers, Pr. Using this initial guess, we can find the initial guess, $G'(0)$ for different Prandtl numbers. Table 1 shows the initial guesses for different Pr [2]. Here, we integrated with a step size of $h = \Delta\eta = 0.1$ using fourth-order Runge-Kutta. Since G is a function of Pr, the values of ∞ vary with Pr i.e., G asymptotically converges at different times for different Pr. These values are also illustrated in Table 1.

Note: All simulations and visualizations were developed in Python using NumPy [1] and Matplotlib [2] libraries respectively.

[1] See Appendix A for details

[2] See Appendix B for details

η	$F(\eta)$	$F'(\eta)$	$F''(\eta)$	$G(\eta)$	$G'(\eta)$
0.0	0.0000000	0.0000000	0.3320573	1.0000000	-0.5766887
0.1	0.0016603	0.0332055	0.3320482	0.9423331	-0.5766089
0.2	0.0066410	0.0664078	0.3319838	0.8846942	-0.5760508
0.3	0.0149415	0.0995986	0.3318094	0.8271548	-0.5745385
0.4	0.0265599	0.1327642	0.3314699	0.7698339	-0.5716052
0.5	0.0414928	0.1658853	0.3309110	0.7128961	-0.5668026
0.6	0.0597347	0.1989373	0.3300791	0.6565496	-0.5597144
0.7	0.0812770	0.2318902	0.3289221	0.6010418	-0.5499728
0.8	0.1061083	0.2647091	0.3273893	0.5466536	-0.5372772
0.9	0.1342130	0.2973540	0.3254326	0.4936921	-0.5214128
1.0	0.1655718	0.3297800	0.3230071	0.4424806	-0.5022694
⋮	⋮	⋮	⋮	⋮	⋮
9.4	7.6792125	1.0000000	0.0000001	0.0000000	0.0000000
9.5	7.7792125	1.0000000	0.0000001	0.0000000	0.0000000
9.6	7.8792125	1.0000000	0.0000000	0.0000000	0.0000000
9.7	7.9792125	1.0000000	0.0000000	0.0000000	0.0000000
9.8	8.0792125	1.0000000	0.0000000	0.0000000	0.0000000
9.9	8.1792125	1.0000000	0.0000000	0.0000000	0.0000000
10.0	8.2792125	1.0000000	0.0000000	0.0000000	0.0000000

Table 2: *Values from numerically integrating the system described in Equations (11–12) using fourth-order Runge-Kutta method. Here, $Pr = 5$ and step size, $h = \Delta\eta = 0.1$. Here, we integrated up to $\infty = 10$.*

From Table 1, we can observe a few characteristics of the initial guess of G'. Firstly, note that the magnitude of $G'(0)$ increases as Pr increases. This can be explained as follows: Pr is inversely related to the thermal diffusivity α and G, the scaled temperature. So, as we increase Pr, we are actually decreasing the thermal diffusivity. This means that heat transfer between the different layers of fluid is small. Thus, we need a larger "slope" for G, which is G', in order to quickly reach the asymptotic value of $G(\infty)$.

Secondly, we noted in Section 3 that when $Pr = 1$, F'' and G' behave similarly. And as expected, when $Pr = 1$, $|F''(0)| = |G'(0)| = 0.33205735$. They have different signs because they asymptotically approach different values.

With $Pr = 5$, we used the guess values from Table 1 to numerically integrate the system in Equations (11–12). With a step size of $h = \Delta\eta = 0.1$, we used the fourth-order Runge-Kutta technique. A few of the values are shown in Table 2. As expected, we correctly reach the boundary conditions. Here, we integrated up to $\infty = 10$.

Now, let $u/U_\infty = F' = 0.98$ and $G = 0.02$, which represent the momentum and thermal

Pr	η_m	η_t
0.1		11.4664115
0.2		8.6071439
0.5		5.8987147
1	4.5144376	4.5144376
2		3.5025953
5		2.5396917
10		2.0063855

Table 3: *Different η values that correspond to the boundary layer conditions $F' = 0.98$ and $G = 0.02$ for different Prandtl numbers Pr.*

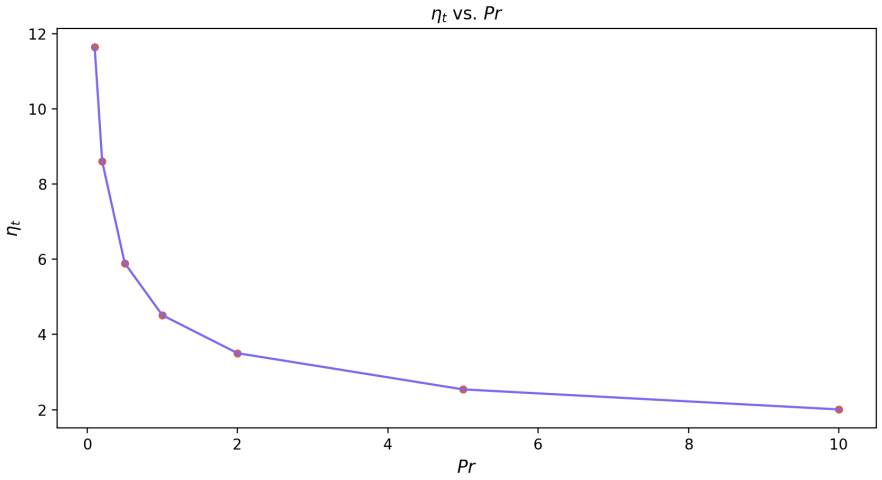

Figure 1: *The blue curve shows how η_t varies with Pr. The red points indicate specific η_t values for different Pr, each of which is calculated in Table 3. These values were used to generate linear approximations for missing values.*

boundary layers respectively. Now, by solving the system for different Prandtl numbers, we can find the value of η that corresponds to the boundary layers. Let η_m correspond to the momentum boundary layer and η_t correspond to the thermal boundary layer.

Although we are not guaranteed to have $\eta_{(\ )}$ that correspond to these exact values of F' and G, we can approximate the values by interpolating a polynomial using the points around the desired values of F' and G. Once again, only η_t varies with Pr and η_m is independent of Pr. Table 3 shows the different $\eta_{(\ )}$ values. Note that $\eta_m = \eta_t$ for $Pr = 1$ as expected from our discussion in Section 3. Figure 1 uses data from Table 3 to envision how η_t varies with the Prandtl number Pr.

By rearranging terms in the similarity transformation, we can obtain dimensionless quantities. In particular, we get the following dimensionless horizontal and vertical velocities:

$$\frac{u}{U_\infty} = F'(\eta)$$
$$\frac{v}{U_\infty}\sqrt{\frac{x}{L}}\sqrt{Re} = \frac{1}{2}\left[\eta F'(\eta) - F(\eta)\right]$$

where $Re = \dfrac{U_\infty L}{\nu}$ is the Reynold's number and L is the length of the plate.

Using our numerically calculated values, we can study the behavior of these dimensionless velocities. These are independent of the Prandtl number Pr. This can be seen in Figure 2. The exact value of η_m corresponding to the boundary layer can be found in Table 3. The vertical velocity is always smaller than the horizontal velocity and begins to increase only after a while. This is because the fluid has no initial vertical velocity and since this is induced, it will always be smaller than the horizontal velocity. Also, notice how both velocities increase with η. This corresponds to the fact that as we go higher in the fluid, the horizontal velocity is greater as it is less affected by friction. And as we go higher, there is more induced vertical velocity as that is where the fluid to "oozes out" in order to conserve mass.

Similarly, we can study the behavior of the dimensionless temperature G as a function of η. Since G is dependent on the Prandtl number Pr, we get different curves for each Pr. Such curves for several different values of Pr are shown in Figure 3. Notice how the curves are stacked on top of other curves with smaller Pr. This is because a smaller Prandtl number indicates a greater thermal diffusivity, α. Therefore, at the same point in the temperature profile, a fluid with greater thermal diffusivity (smaller Pr) will have a greater temperature because heat transfer is faster. In Figure 3 each curve's η_t value that corresponds to the boundary layer thickness ($G = 0.02$) is labeled. The exact values can be found in Table 3.

Now that we have a good idea of how the model behaves, and the intuition behind its behavior, we can begin studying the momentum and thermal boundary layers.

Since η_m is the value of η that corresponds to the momentum boundary layer thickness, the y value that defines η_m is also the momentum boundary layer, δ_m. Therefore, we have,

$$\eta_m = \frac{\delta_m}{\sqrt{\frac{\nu x}{U_\infty}}}$$
$$\implies \delta_m \frac{\sqrt{Re}}{L} = \eta_m \sqrt{\frac{x}{L}} \tag{18}$$

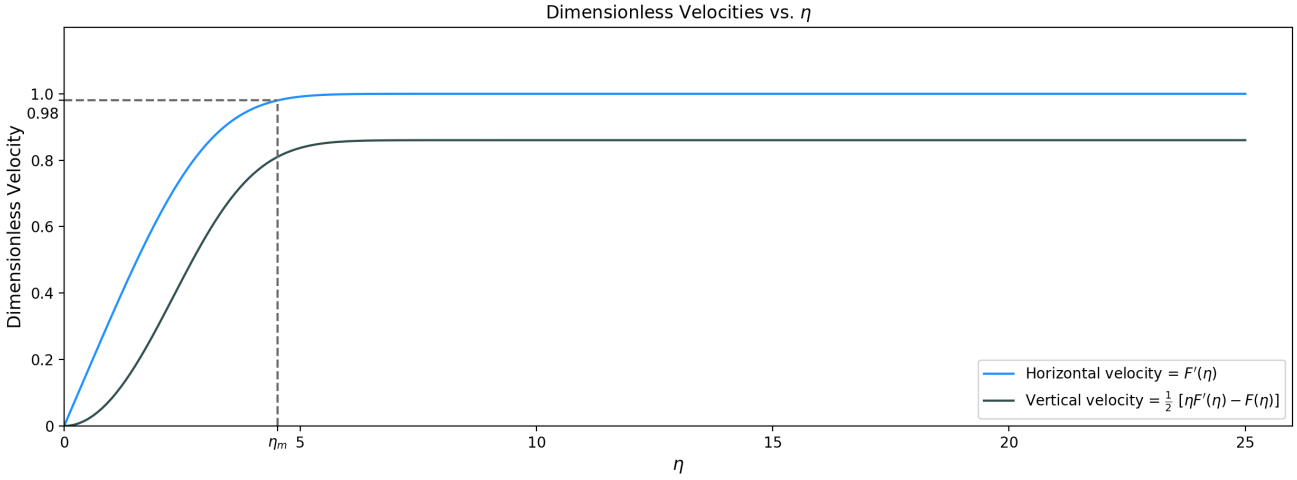

Figure 2: *The behavior of dimensionless velocities. The blue line shows the horizontal velocity and the grey line shows the vertical velocity. The η value corresponding to the boundary layer is also marked. The exact value of η_m can be found in Table 3.*

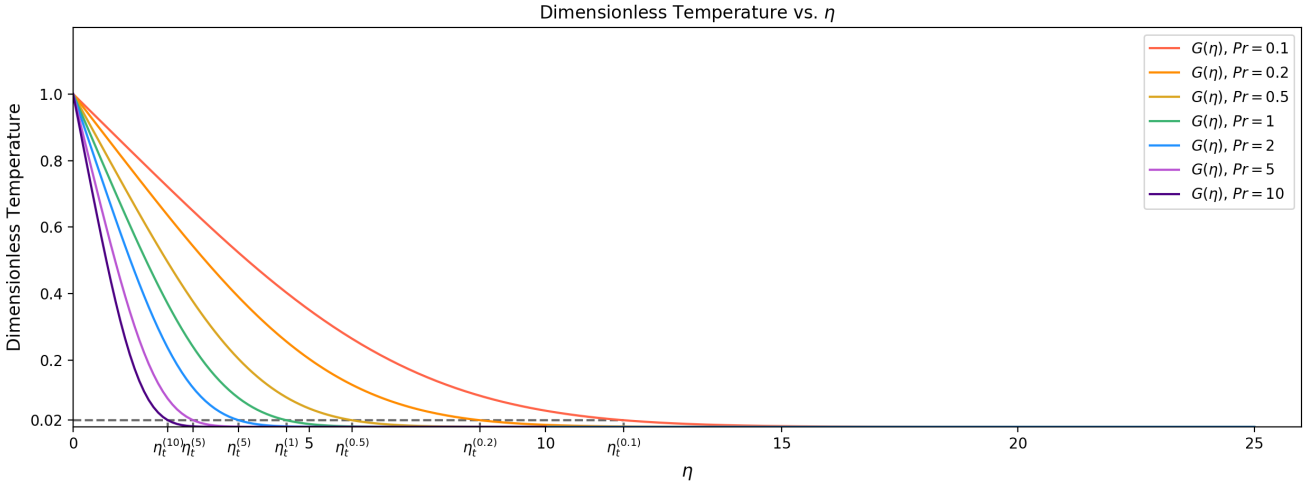

Figure 3: *The behavior of dimensionless temperature G. The different colored curves correspond to different values of Pr. Each curve's $\eta_t^{(Pr)}$ that corresponds to the boundary layer thickness is also labeled. The exact values of each η_t can be found in Table 3.*

where Re is the Reynold's number and L is the length of the plate. Similarly, we can show that the thermal boundary layer δ_t, is defined as,

$$\implies \delta_t \frac{\sqrt{Re}}{L} = \eta_t \sqrt{\frac{x}{L}} \tag{19}$$

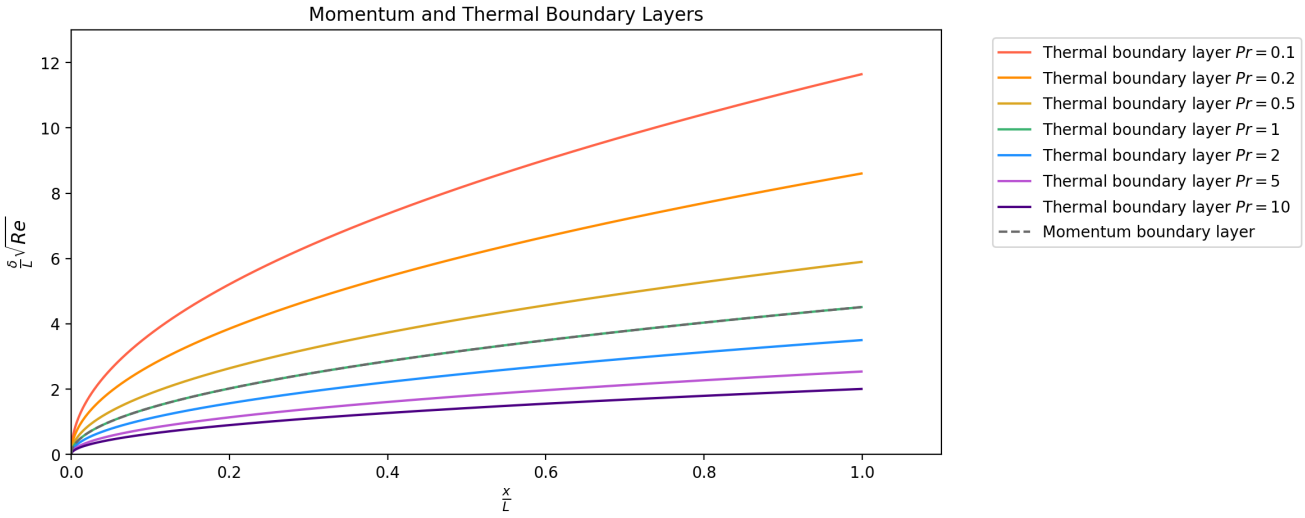

Figure 4: *The momentum and thermal boundary layer of the fluid. The dashed grey curve represents the momentum boundary layer. Differently colored solid curves correspond to thermal boundary layers for different Prandtl numbers Pr.*

Figure 4 shows the momentum boundary layer δ_m as a dashed grey curve. As expected, the the boundary layer increases as the fluid flows further. This is because as the fluid moves across the plate, more of it will also slowly lose momentum, which increases the height where the fluid still retains its original horizontal velocity.

Figure 4 shows the thermal boundary layer δ_t. Since η_t is dependent on Pr, we have different boundary layers corresponding to different Pr. A smaller Pr (greater thermal diffusivity) means that heat travels faster between layers of the fluid. So, we would need to go higher along the fluid's temperature profile to reach the first layer that has the same temperature. This explains why curves with smaller Pr are stacked on curves with higher Pr.

Notice that the thermal boundary layer for $Pr = 1$ and the momentum boundary layer are the exact same curve. This is to be expected from our discussion in Section 3. To distinguish them, the momentum boundary layer is shown as a dashed curve.

6 Conclusion

The answer to the great question of life, the universe and everything is 42.

– Douglas Adams

We have studied, in detail, how a fluid behaves as it flows along a heated plate. We used the law of conservation of mass, momentum and energy to design a system of partial differential equations. We transformed this into a boundary value problem of ordinary differential equations. We then used root finding techniques to convert this into an initial value problem. By numerically solving this problem, we studied two different properties of the fluid.

Firstly, due to friction, the fluid sticks to the plate and is gradually slowed down. This means that as the fluid flows further along the plate, we need to travel farther from the plate to reach a point in the fluid that has the same initial velocity. This point, that has constant velocity as the fluid travels further, is called the momentum boundary layer. This curve is shown by the gray dashed line in Figure 4.

Secondly, due to the temperature difference, heat diffuses along the fluid. Similar to the momentum boundary layer, we can trace a point in the fluid that has constant temperature. This is called the thermal boundary layer. Several different thermal boundary layers, each corresponding to fluids with different thermal properties, are shown by solid lines in Figure 4.

This model has several applications, including heat sinks, thermal behavior of jet turbine engines, heat diffusion from aircraft, and many other situations where a fluid flows over a heated surface. For instance, in a heat sink, it is optimal for the fluid that cools the heat sink to reach the temperature of the heat sink throughout the volume of the fluid as it exits the heat sink. We can study this by making small changes to our model to accommodate the complexity of the heat sink's design. Another application is designing wings to make an aircraft as energy efficient as possible. The only modification we must make to our model, to study this, is combining multiple plates with different positions to approximate the wing.

References

[1] T. E. Oliphant, *Guide to NumPy*, vol. 1. Dec 2006.

[2] J. D. Hunter, "Matplotlib: A 2D graphics environment," *Computing In Science & Engineering*, vol. 9, no. 3, pp. 90–95, 2007.

[3] R. L. Burden and J. D. Faires, *Numerical Analysis*. Cengage Learning, 9 ed., Aug 2010.

A Estimating $F''(0)$

We have a root finding problem where we need to find $F''(0)$ such that $F'(\infty) = 1$. Essentially, we need to begin with an initial guess for $F''(0)$, integrate the system to ∞ to find $F'(\infty)$. Then we correct our guess. We eventually stop when our solution reaches a desired tolerance value.

Here, we used the Bisection algorithm to estimate $F''(0)$. We start with two guesses a and b that straddle $F'(\infty) = 1$. We take their average and discard the farther point. For convergence, we stop iterating when $|F'(\infty) - 1| \leq 10^{-9}$. Using $a = 0$ and $b = 1$, we find that $F''(0) = 0.33205735$. A few values are illustrated in Table 4.

Iteration (i)	$F''_{(i)}(0)$
1	0.50000000
2	0.25000000
3	0.37500000
4	0.31250000
5	0.34375000
⋮	⋮
26	0.33205734
27	0.33205735

Table 4: *Estimating $F''(0)$ using bisection algorithm with $a = 0$, $b = 1$.*

B Estimating $G'(0)$

Similar to how we found $F''(0)$ in Appendix A, we have a root finding problem where we want to find $G'(0)$ such that $G(\infty) = 0$. However, this depends on the Prandtl number Pr.

Once again, we used the Bisection algorithm. We declare convergence when $|G(\infty) - 0| \leq 10^{-9}$. Using the initial guess $F''(0)$ we found in Appendix A, and $a = -2$, $b = 4$, we found different estimates for $G'(0)$ for different Pr. These values are illustrated in Table 1. The estimates we get during the bisection algorithm are illustrated in Tables 5-11

Iteration (i)	$G'_{(i)}(0)$
1	1.00000000
2	-0.50000000
3	0.25000000
4	-0.12500000
5	-0.31250000
⋮	⋮
28	-0.14002942
29	-0.14002943

Table 5: *Estimating* $G'(0)$ *using bisection algorithm with* $a = -2$, $b = 4$. *Here,* $Pr = 0.1$.

Iteration (i)	$G'_{(i)}(0)$
1	1.00000000
2	-0.50000000
3	0.25000000
4	-0.12500000
5	-0.31250000
⋮	⋮
31	-0.18409610
32	-0.18409610

Table 6: *Estimating* $G'(0)$ *using bisection algorithm with* $a = -2$, $b = 4$. *Here,* $Pr = 0.2$.

Iteration (i)	$G'_{(i)}(0)$
1	1.00000000
2	-0.50000000
3	0.25000000
4	-0.12500000
5	-0.31250000
⋮	⋮
29	-0.25929357
30	-0.25929356

Table 7: *Estimating* $G'(0)$ *using bisection algorithm with* $a = -2$, $b = 4$. *Here,* $Pr = 0.5$.

Iteration (i)	$G'_{(i)}(0)$
1	1.00000000
2	-0.50000000
3	0.25000000
4	-0.12500000
5	-0.31250000
⋮	⋮
30	-0.33205734
31	-0.33205735

Table 8: *Estimating* $G'(0)$ *using bisection algorithm with* $a = -2$, $b = 4$. *Here,* $Pr = 1$.

Iteration (i)	$G'_{(i)}(0)$
1	1.00000000
2	-0.50000000
3	0.25000000
4	-0.12500000
5	-0.31250000
⋮	⋮
27	-0.42230816
28	-0.42230814

Table 9: *Estimating* $G'(0)$ *using bisection algorithm with* $a = -2$, $b = 4$. *Here,* $Pr = 2$.

Iteration (i)	$G'_{(i)}(0)$
1	1.00000000
2	-0.50000000
3	-1.25000000
4	-0.87500000
5	-0.68750000
⋮	⋮
27	-0.57668869
28	-0.57668871

Table 10: *Estimating* $G'(0)$ *using bisection algorithm with* $a = -2$, $b = 4$. *Here,* $Pr = 5$.

Iteration (i)	$G'_{(i)}(0)$
1	1.00000000
2	-0.50000000
3	-1.25000000
4	-0.87500000
5	-0.68750000
⋮	⋮
27	-0.72814052
28	-0.72814050

Table 11: *Estimating $G'(0)$ using bisection algorithm with $a = -2$, $b = 4$. Here, $Pr = 10$.*